The Orthogonal Analysis of Tensor Decomposition for Multisubject FMRI Analysis

Biao Wang, Bingjing Cui*, Yipu Zhang

School of electronics and control engineering, Chang' an University, Xi'an, China

wangbiao@chd.edu.cn
2020132049@chd.edu.cn
zyipu@chd.edu.cn

Abstract. As neuroimaging technology matures, high-dimensional biomedical data is gradually applied to research. Location of activated regions from multi subject fMRI data is the foundation for exploring functional brain tissue in neuroscience. However, most of the methods ignore the multi-way nature of the data and the crosstalk or overlap in the spatiotemporal representation of the located components. To this end, we propose an orthogonal analysis method based on sparse decomposition of tensors. Specifically, a novel sparse tensor decomposition with orthogonality is designed to decompose the tensor into three matrices (subject, space and time), which can extract common components across subjects and reduce components. To verify the effectiveness of the proposed model, our model is compared with CANDECOMP/PARAFAC decomposition (CPD), tensor independent component analysis (Tensor ICA), independent component analysis, group independent component analysis (GICA), and method based on nonnegative matrix decomposition using simulated data. The experimental results show that our proposed model can effectively locate the activation area and activation time as well as improve the calculation speed of decomposition. Moreover, the components decomposed by our model simply and efficiently represent multi-subject fMRI data which facilitates interpretation and optimization of group fMRI studies.

Keywords: fMRI, tensor decomposition, functional network, component, multi subject.

1 Introduction

Functional magnetic resonance imaging(fMRI) is an emerging imaging modality for studying human neural brain tissue. Its principle is to use magnetic resonance imaging to measure hemodynamic changes caused by neuronal activity. Due to the non-invasive and safety features of fMRI, it is widely used in research. Researchers found that human brain always has brain activity [1]. Locating brain activated regions is defined as blind source separation (BSS), where sources include spatial maps (SMs) and time

H. Wu et al. (Eds.): CSIEDE 2022, ACSR 103, pp. 711–720, 2022.
https://doi.org/10.2991/978-94-6463-108-1_79

courses (TCs) [2]. Matrix-based techniques are the most common method solving blind source analysis.

Gael Varoquaux et al [3] and Harrison et al [4] decompose fMRI data with multi subject dictionary learning approach and assume that the decomposed components follow a Gaussian distribution or delta Gaussian distribution. JingLei Lv et al [5] compare the two hypotheses and incorporate sparsity into the dictionary learning decomposition. Subsequently, C.F. Beckmann et al [6] studied the fMRI data with independent component analysis (ICA) to obtain the SMs and TCs. Nevertheless, some researchers have proposed that decomposing the mixed data of a group of subjects can obtain more robust independent components (ICs) [7]. Therefore, Calhoun et al [8] proposed group ICA (GICA) to decompose functional data, while it is a challenging thing to decompose the components of subjects from mixed data. To address this problem, we generally use heuristic techniques such as back-reconstruction and dual regression. Afterwards, Hongming Li et al [7] proposed a hypothesis that defined negative loading as an anticorrelation signal and believed that we difficultly explain the biological significance of time course of a component with positive and negative loading. However, these methods based on matrix factorization have shortcomings in utilizing the inherent multi way of fMRI data [9]. In contrast, the tensor analysis model retains this feature. The tensor analysis model generates unique representation under mild conditions [10], improves the ability of extracting spatiotemporal models of interest [11][12] and facilitates neurophysiologically meaningful interpretations [10]. And the advantages of locating sources with tensor analysis methods over matrix-based methods have been proven [2]. Tensor methods for multi subject fMRI data include CANDECOMP/PARAFAC decomposition (CPD) by Bhaskar Sen et al [11] and tensor independent component analysis proposed by C.F. Beckmann and S.M. Smith [12].

However, neither CPD nor Tensor ICA consider component redundancy and component crosstalk. To this end, we propose our model based on CPD and add the following items: 1) the group sparsity term is added in the subject matrix to remove the redundant components of each subject; 2) in order to reduce the crosstalk between components; 3) the parsimonious regularization term is increased in temporal matrix, so that we extract the activated time points of each component.

2 Materials and Methods

2.1 Notion

The model of tensor-based analysis is characterized by the following:

$$x_{\mathrm{ijk}} = \sum_{\mathrm{r}}^{\mathrm{R}} a_{\mathrm{ir}} b_{jr} c_{kr} + \varepsilon_{ijk} \tag{1}$$

where ε is additional noise with a Gaussian distribution $N(0, \sigma I)$. The objective function of this tensor-based model is as follow:

$$\min_{\mathbf{A},\mathbf{B},\mathbf{C}} \sum_{i,j,k} \| x_{ijk} - \sum_{r=1}^{R} a_{ir} b_{jr} c_{kr} \| \tag{2}$$

Here, $\mathbf{A} \in \mathbb{R}^{I \times R}$, $\mathbf{B} \in \mathbb{R}^{J \times R}$, $\mathbf{C} \in \mathbb{R}^{K \times R}$ and the matrices containing R components in subject, spatial and temporal matrices subscribed as column. The tensor χ in the formula (2) can be matrixed by tensor unfolding according to mode-n:

$$\mathbf{X}_{(1)} = \mathbf{A}\left(\mathbf{C} \odot \mathbf{B}\right)^{\mathrm{T}}, \mathbf{X}_{(1)} \in \mathbb{R}^{I \times JK} \tag{3}$$

$$\mathbf{X}_{(2)} = \mathbf{B}\left(\mathbf{C} \odot \mathbf{A}\right)^{\mathrm{T}}, \mathbf{X}_{(2)} \in \mathbb{R}^{J \times KI} \tag{4}$$

$$\mathbf{X}_{(3)} = \mathbf{C}\left(\mathbf{B} \odot \mathbf{A}\right)^{\mathrm{T}}, \mathbf{X}_{(3)} \in \mathbb{R}^{K \times JI} \tag{5}$$

where $\odot$ stands for Khatri-Rao product. $\mathbf{X}_{(n)}$ is the matrix of the tensor unfolding in the n-th dimension that reduce the calculation difficulty. The objective functions can be rewritten as:

$$\min_{\mathbf{A}} \| \mathbf{X}_{(1)} - \mathbf{A}\left(\mathbf{C} \odot \mathbf{B}\right)^{\mathrm{T}} \| \tag{6}$$

$$\min_{\mathbf{B}} \| \mathbf{X}_{(2)} - \mathbf{B}\left(\mathbf{C} \odot \mathbf{A}\right)^{\mathrm{T}} \| \tag{7}$$

$$\min_{\mathbf{C}} \| \mathbf{X}_{(3)} - \mathbf{C}\left(\mathbf{B} \odot \mathbf{A}\right)^{\mathrm{T}} \| \tag{8}$$

2.2 Algorithms and model

Considering the characteristics of the three dimensions of tensor, our method built upon CPD and enhanced three kinds of constraints. First, $L_{2,1}$-norm penalty term is added in subject matrix $\mathbf{A}$, which makes each column of the transposed matrix of $\mathbf{A}$ sparse and eliminates redundant components to retain common components across subjects. Secondly, orthogonality term is adopted to spatial matrix $\mathbf{B}$, so that the correlation and crosstalk between components are reduced. Thirdly, enhancing L_1 sparse term in the temporal matrix $\mathbf{C}$ removes redundant time points through non-zero values and extracts important time points. The specific explanation is shown in Figure 1. The proposed model is as follows:

$$\min_{\mathbf{A},\mathbf{B},\mathbf{C}} \frac{1}{2} \| \chi - \mathbf{A},\mathbf{B},\mathbf{C} \|_F^2 + \lambda_1 \| \mathbf{A}^{\mathrm{T}} \|_{2,1} + \frac{\lambda_2}{2} \| \mathbf{B}^{\mathrm{T}}\mathbf{B} - \mathbf{I} \|_F^2 + \lambda_3 \| \mathbf{C} \|_1 \tag{9}$$

$$s.t. \sum_{j=1}^{J} b_{jr}^2 = 1, \sum_{k=1}^{K} c_{kr}^2 = 1, \forall r \in \{1, 2, \ldots, R\}$$

Here, λ_1, λ_2 and λ_3 are positive regularization parameters that balance the data fitting, the degree of sparsity and orthogonality. In addition, constraints are imposed on the

matrices $\mathbf{B}$ and $\mathbf{C}$. In particularly, in each iteration, normalizing each column of $\mathbf{B}$ and $\mathbf{C}$ avoids matrix $\mathbf{A}$ being too large or too small.

According to joint model, the objective function can be rewritten as:

$$\Gamma := \frac{1}{2} \| \mathbf{X}_{(1)} - (\mathbf{B} \odot \mathbf{C}) \cdot \mathbf{A}^{\mathrm{T}} \|_F^2 + \lambda_1 \| \mathbf{A}^{\mathrm{T}} \|_{2,1} + \frac{\lambda_2}{2} \| \mathbf{B}^{\mathrm{T}} \mathbf{B} - \mathbf{I} \|_F^2 + \lambda_3 \| \mathbf{C} \|_1 \tag{10}$$

or

$$\Gamma := \frac{1}{2} \| \mathbf{X}_{(2)} - (\mathbf{C} \odot \mathbf{A}) \cdot \mathbf{B}^{\mathrm{T}} \|_F^2 + \lambda_1 \| \mathbf{A}^{\mathrm{T}} \|_{2,1} + \frac{\lambda_2}{2} \| \mathbf{B}^{\mathrm{T}} \mathbf{B} - \mathrm{I} \|_F^2 + \lambda_3 \| \mathbf{C} \|_1 \tag{11}$$

or

$$\Gamma := \frac{1}{2} \| \mathbf{X}_{(3)} - (\mathbf{A} \odot \mathbf{B}) \cdot \mathbf{C}^{\mathrm{T}} \|_F^2 + \lambda_1 \| \mathbf{A}^{\mathrm{T}} \|_{2,1} + \frac{\lambda_2}{2} \| \mathbf{B}^{\mathrm{T}} \mathbf{B} - \mathbf{I} \|_F^2 + \lambda_3 \| \mathbf{C} \|_1 \tag{12}$$

The objective functions respectively take the partial derivatives of the matrices $\mathbf{A}$, $\mathbf{B}$ and $\mathbf{C}$. The following results are obtained:

$$\frac{\partial \Gamma}{\partial \mathbf{A}} = \left(\mathbf{A} \left(\mathbf{C} \odot \mathbf{B} \right)^{\mathrm{T}} - \mathbf{X}_{(1)} \right) \left(\mathbf{C} \odot \mathbf{B} \right) + \lambda_1 \mathbf{A} \boldsymbol{\Theta} \tag{13}$$

$$\frac{\partial \Gamma}{\partial \mathbf{B}} = \left(\mathbf{B} \left(\mathbf{C} \odot \mathbf{A} \right)^{\mathrm{T}} - \mathbf{X}_{(2)} \right) \left(\mathbf{C} \odot \mathbf{A} \right) + 2\lambda_2 \left(\mathbf{B} \mathbf{B}^{\mathrm{T}} - \mathbf{I} \right) \mathbf{B} \tag{14}$$

$$\frac{\partial \Gamma}{\partial \mathbf{C}} = \left(\mathbf{C} \left(\mathbf{B} \odot \mathbf{A} \right)^{\mathrm{T}} - \mathbf{X}_{(3)} \right) \left(\mathbf{B} \odot \mathbf{A} \right) + \lambda_3 sgn(\mathbf{C}) \tag{15}$$

where $sgn(\bullet)$ represents sign function. $\Theta \in \mathbb{R}^{R \times R}$ is a diagonal matrix with elements $1/\| a_r \|_2$ and $\mathbf{A}\boldsymbol{\Theta} = \partial(\| \mathbf{A}^{\mathrm{T}} \|_{2,1}) / \partial \mathbf{A}$. The formulas after partial derivative are settled to zero to get the updated formulas of $\mathbf{A}$ and $\mathbf{C}$. The updated formulas are as follows:

$$\mathbf{A}^{t+1} = \frac{\mathbf{X}_{(1)} \left(\mathbf{C}^t \odot \mathbf{B}^t \right)}{\left(\mathbf{C}^t \odot \mathbf{B}^t \right)^{\mathrm{T}} \left(\mathbf{C}^t \odot \mathrm{B}^t \right) + \lambda_1 \boldsymbol{\Theta}} \tag{16}$$

$$\mathbf{C}^{t+1} = \frac{\mathbf{X}_{(3)} \left(\mathbf{B}^t \odot \mathbf{A}^t \right) - \lambda_3 sgn\left(\mathbf{C}^t \right)}{\left(\mathbf{B}^t \odot \mathbf{A}^t \right)^{\mathrm{T}} \left(\mathbf{B}^t \odot \mathbf{A}^t \right)} \tag{17}$$

$$\mathbf{B}^{t+1} = \mathbf{B}^t - \gamma \left[\left(\left(\mathbf{C}^t \odot \mathbf{A}^t \right) \mathbf{B}^t - \mathbf{X}_{(2)} \right) \left(\mathbf{C}^t \odot \mathbf{A}^t \right)^{\mathrm{T}} + 2\lambda_2 \left(\mathbf{B}^t \mathbf{B}^{t\mathrm{T}} - \mathbf{I} \right) \mathbf{B}^t \right] \tag{18}$$

Table 1. The pseudocode of the proposed optimization algorithm (owner-draw)

Algorithm 1 The orthogonal analysis of tensor decomposition

Input: χ :functional data of all subjects; $\lambda_1, \lambda_2, \lambda_3, R$

Output: $\mathbf{A}$, $\mathbf{B}$ and $\mathbf{C}$

Alternative updates:

for t = 1 to mixites **do**

update $\mathbf{A}$ as in Eq. (16)

update $\mathbf{C}$ as in Eq. (17)

for r = 1 to R **do**

$c_r^t = c_r^t / \| c_r^t \|_1$

end for

update $\mathbf{B}$ as in Eq. (17)

for r = 1 to R **do**

$b_r^t = b_r^t / \| b_r^t \|_1$

end for

until converge

end for

Here, γ is learning rate. t represents the t -th iteration. The update process is shown in Algorithm 1.

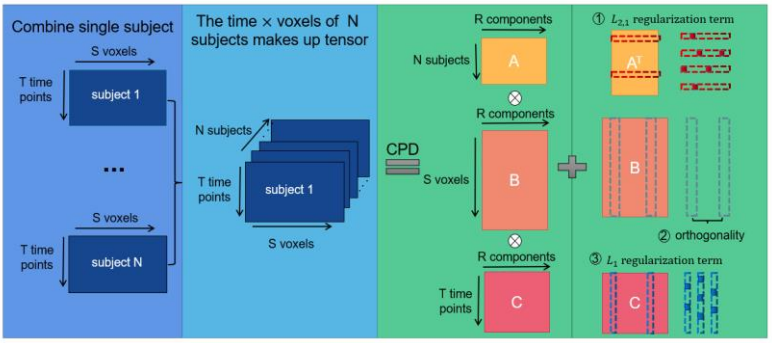

Fig. 1. Schematic diagram of joint model based on CPD (owner-draw)

2.3 Performance evaluation

Model performance is evaluated using the accuracies between the components in the decomposed temporal and spatial matrices and the sources corresponding to the ground truth in time and space [2]. There are two types of model accuracy: spatial accuracy (SM accuracy) and temporal accuracy (TC accuracy). The spatial accuracy is calculated by the activated region and ground truth according to formula (19). The temporal accuracy is calculated by the activated time and ground truth according to formula (20). The formulas for calculating $error_{SM}$ and $error_{TC}$ are as follows:

$$error_{\mathrm{SM}} = |\, corr(\mathbf{B}_r, \mathbf{B}_{\mathrm{SM}n}) \,| \tag{19}$$

$$error_{\mathrm{TC}} = |\, corr(\mathbf{C}_r, \mathbf{C}_{\mathrm{TC}n}) \,| \tag{20}$$

Here, $corr(\bullet)$ means to calculate the Pearson correlation coefficient. Where $r = 1, 2, \ldots, R$, $n = 1, 2, \ldots, N$. R is the number of components of the decomposed matrix using MELODIC of FSL [13]. N is the number of components. $\mathbf{B}_r$ represents the r-th column of the decomposed spatial matrix. $\mathbf{B}_{\mathrm{SM}n}$ represents the n-th column of the spatial ground truth. Similarly, the r-th column of the decomposed temporal matrix is denoted by $\mathbf{C}_r$ and $\mathbf{C}_{\mathrm{TC}n}$ is the n-th column of the temporal ground truth.

3 Result

3.1 Synthetic data

In this work, simulation dataset is generated by SimTB toolbox in MATLAB [14], in which the dataset is consists of 100 subjects and each of subject has 50 2D images with 50×50 voxels, composed by 25 different components. When generating data, there are not only individual differences in spatial translation, rotation and spread between subjects, but also Rician noise and random contrast in the range of 0.1 to 2 are added, so that all signals between subjects are inconsistent in time and space.

3.2 Parameter Selection and Experiment Result

The proposed method has three positive regularization terms including λ_1, λ_2 and λ_3. Using the grid search method, exacting parameter values can be adjusted by accuracies between the components of the temporal matrix and the spatial matrix and the sources corresponding to the ground truth in time and space within the range of parameters. The results of parameter adjustment under SM precision and TC precision are shown in Fig 2. The tuning ranges of the three parameters of our model are: $\lambda_1 \in \{5\times10^{-4}, 1\times10^{-3}, 5\times10^{-3}, 1\times10^{-2}, 2\times10^{-2}, 3\times10^{-2}, 4\times10^{-2}, 5\times10^{-2}, 6\times10^{-2}, 7\times10^{-2}, 8\times10^{-2}, 9\times10^{-2}, 0.1, 1\}$, $\lambda_2 \in \{3\times10^{-3}, 4\times10^{-3}, 5\times10^{-3}, 6\times10^{-3}, 7\times10^{-3}, 8\times10^{-3}, 9\times10^{-3}\}$ and $\lambda_3 \in \{1\times10^{-2}, 1\times10^{-1}, 1, 5, 10, 15, 20, 25, 30, 35, 40, 45, 50, 70, 100\}$. Finally our proposed model achieves the best time course accuracy and spatial map accuracy at $\lambda_1 = 0.005$, $\lambda_2 = 0.007$ and $\lambda_3 = 20$.

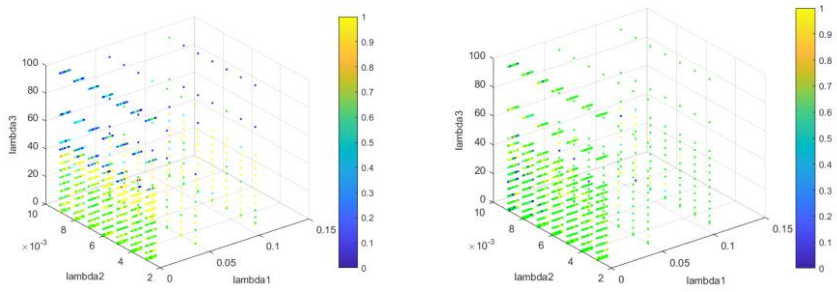

Fig. 2. The accuracy of our model in different parameter ranges. (a) Time course accuracy within parameter range. (b) Spatial map accuracy within the parameter range (owner-draw)

In experiments, the proposed model is compared with 5 models, such as non-negative matrix factorization based sparse model analysis (Sparse NMF is used to represent the method) in Reference [7], ICA, group ICA, CPD and Tensor ICA. Specifically, the mean and standard deviation of the model accuracy are obtained by repeating the decomposition process 20 times for each model. Fig. 3 shows the time course accuracy and spatial map accuracy for all models. In Figure 3, Sparse NMF1 means that Sparse NMF performs model analysis on subject level fMRI data, while Sparse NMF performs model analysis under pooled data of a group of subject fMRI data, which is denoted by Sparse NMF2. As shown in Table 1, the algorithmic performance of the six models on synthetic data is summarized.

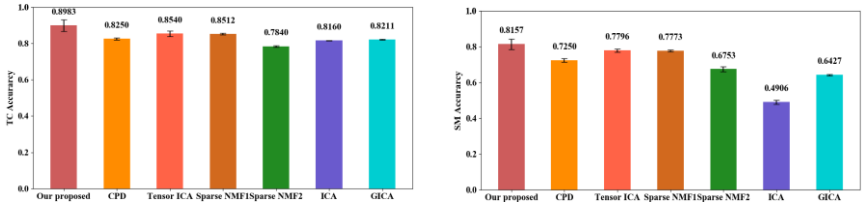

Fig. 3. Time course accuracy and spatial map accuracy for all models. (a) Time courses accuracy of all models. (b) Spatial maps accuracy of all models. (owner-draw)

Table 2. Time course accuracy (mean ± std) and spatial map accuracy (mean ± std) of the six models (owner-draw)

Model	TC Accuracy	SM Accuracy
the proposed method	**0.8983 ± 0.0317**	**0.8157 ± 0.0293**
CPD	0.8250 ± 0.0063	0.7250 ± 0.0109
Tensor ICA	0.8540 ± 0.0157	0.7796 ± 0.0081
Sparse NMF1	0.8512 ± 0.0048	0.7773 ± 0.0057
Sparse NMF2	0.7840 ± 0.0047	0.6753 ± 0.0145
ICA	0.8160 ± 0.0143	0.4906 ± 0.0114
GICA	0.8211 ± 0.0013	0.6427 ± 0.0037

The temporal and spatial accuracy of our model are 0.8983 ± 0.0317 and 0.8157 ± 0.0293. From the above, it can be concluded that our model is superior to several other models. Our model achieves TC accuracy of 0.9652 and SM accuracy of 0.8537 in 20 decomposition runs. We also compare the computational speed of all models, which is the average time of running the decomposed model 5 times in full on multi-subject fMRI simulation data. Where Sparse NMF2 and GICA are decomposed by concatenating data along the temporal dimension with a group of subject fMRI data. The data size used by other models except Sparse NM2 and GICA is $100 \times 2500 \times 50$, and the dimension is expressed as subject $\times$ voxels $\times$ time. The calculation speed of each model is shown in Table 2. Both the Sparse NMF2 and GICA algorithms were run 5 times on pooled data and the average time was calculated.

Table 3. Mean computation time of each method in seconds (s) (owner-draw)

Data	Model	Computing Speed
subject × voxels × time ($100 \times 2500 \times 50$)	Our proposed method	203.818875 s
	CPD	363.371302 s
	Tensor ICA	265.816607 s
	Sparse NMF1	753.995162 s
	ICA	646.135286 s
a group of subjects ($(2500 * 10) \times 50$) (number of subjects = 10)	Sparse NMF2	267.358157 s
	GICA	353.995162 s

3.3 Analysis and discussion

To analyze TCs and SMs from multi-subject fMRI data, matrix-based methods are often employed for this problem. But the essence of matrix representation is the decomposition of bilinear data, by decomposing single subject data or pooled data of multiple subjects in time or space [15], such as ICA, GICA and Sparse NMF. These methods risk losing the multi-way nature and interactions in the data.

However, tensor analysis methods combine the compression ratio and multidimensional nature of the data, such as our proposed model, CPD and Tensor ICA. But neither of two tensor methods considers the crosstalk between components and the component redundancy in the decomposition matrixes. Unlike other tensor analysis methods, our proposed orthogonal model based on tensor sparse decomposition for analyzing multi-subject fMRI data adds stronger constraints on the three dimensions of the tensor. Our proposed orthogonal model based on tensor sparse decomposition for analyzing multi-subject fMRI data adds stronger constraints on tensor dimensions. Our model reduces linear correlation and crosstalk between components by adding orthogonality constraints to the activation regions. Then, group sparsity is added to the subject matrix to preserve important and common components across subjects. Finally, L_1 regularization term is enhanced at the activated time to eliminate redundant time points of components and extract the activated components in time.

In summary, there are three contributions in this paper. First, we consider the multi-way nature of fMRI in the data and adopt the tensor analysis method. Secondly, we add orthogonality and two kinds of sparse terms based on CPD, which improves the robustness of model assumptions and prevents overfitting. Finally, our model outperforms other models in terms of TCs and SMs accuracy and computational speed, indicating that our decomposition improves the accuracy of tensor decomposition and effectively express multi-subject fMRI data.

4 Conclusion

In this paper, we propose an orthogonal analysis model based on sparse tensor decomposition to identify activation regions and activation times using multi-subject fMRI data. In particularly, the fMRI data of multiple subjects is regarded as a tensor of subject by space by time, which is decomposed founding on CPD and the crosstalk between components is reduced by orthogonality. Moreover, combining different sparse terms on cornerstone of orthogonality extracts activated components across subjects and activated components at a certain time point, which further improves model accuracy and prevents model overfitting. We verify the performance of our algorithm on simulated data and compare it with five other models. The experimental results show that our model can simply and effectively express multi-subject fMRI data. While ensuring high accuracy, the proposed model improves the calculation speed of matrix-based methods for both individual and group-level analysis, which further demonstrates that our model is helpful for explaining and optimizing population fMRI studies.

5 References

1. M. A. Lindquist. The statistical analysis of fMRI data[J]. Statistical Science, 2008,23(4):439-464.
2. Chatzichristos C, Kofidis E, Morante M et al. Blind fMRI source unmixing via higher-order tensor decompositions[J]. Neurosci Methods, 2019, 315(1):17-47.
3. Gael Varoquaux, Alexandre Gramfort, Fabian Pedregosa et al. Multi-subject dictionary learning to segment an atlas of brain spontaneous activity[J]. Inf Process Med Imaging, 2011, 22(1): 562-73.
4. Harrison SJ, Woolrich MW, Robinson EC et al. Large-scale probabilistic functional modes from resting state fMRI[J]. NeuroImage, 2015, 109(1): 217-231.
5. Jinglei Lv, Xi Jiang, Xiang Li et al. Sparse representation of whole-brain fMRI signals for identification of functional networks[J]. Med Image Anal, 2015, 20(1): 112-34.
6. C.F. Beckmann and S.M. Smith. Probabilistic independent component analysis for functional magnetic resonance imaging[J]. IEEE Transactions on Medical Imaging, 2004, 23(2): 137-152.
7. Hongming Li, Theodore D. Satterthwaite, Yong Fan. Large-scale sparse functional networks from resting state fMRI[J]. Neuroimage, 2017, 156(1): 1-13.
8. Calhoun VD, Liu J, Adali T. A review of group ICA for fMRI data and ICA for joint inference of imaging, genetic, and ERP data[J]. NeuroImage, 2009, 45(1): 163-172.

9. C. Chatzichristos, M. Vandecapelle, E. Kofidis et al. Tensor-based Blind fMRI Source Separation Without the Gaussian Noise Assumption—A β-Divergence Approach[J]. IEEE Global Conference on Signal and Information Processing (GlobalSIP), 2019: 1-5.
10. N. Sidiropoulos and R. Bro. On the uniqueness of multilinear decomposition of N-way arrays[J]. Chemometrics, 2000, 14(3): 229-239.
11. B. Sen and K. K. Parhi. Constrained Tensor Decomposition Optimization with Applications To fMRI Data Analysis[C]// 2018 52nd Asilomar Conference on Signals, Systems, and Computers, 2018: 1923-1928,
12. Beckmann CF, Smith SM. Tensorial extensions of independent component analysis for multisubject FMRI analysis[J]. Neuroimage, 2005, 25(1): 294-311.
13. A. H. Andersen and W. S. Rayens. Structure-seeking multilinear methods for the analysis of fMRI data[J]. NeuroImage, 2004, 22(2): 728-739.
14. Erhardt EB, Allen EA, Wei Y et al. SimTB, a simulation toolbox for fMRI data under a model of spatiotemporal separability[J]. Neuroimage, 2012, 59(4): 4160-4167.
15. Andersen AH, Rayens WS. Structure-seeking multilinear methods for the analysis of fMRI data[J]. Neuroimage, 2004, 22(2):728-39.